Nonsteady-State Kinetics of Droplet Growth in Cloud Physics[1]

NORBERT NIX[2] AND NORIHIKO FUKUTA

Denver Research Institute, University of Denver, Colorado 80210

(Manuscript received 20 November 1973, in revised form 27 January 1974)

ABSTRACT

The nonsteady-state kinetics of droplet growth or evaporation is studied theoretically for two types of changing boundary conditions: changes in the distant environment, and changes at the droplet surface. The treatment assumes Maxwellian boundary conditions at the droplet surface. The nonsteady-state kinetics during rapid environmental changes is reviewed, and compared with the simulation of the process obtained by applying the quasi-steady-state theory in a stepwise manner. A method for estimating the errors arising from use of the quasi-steady-state theory to determine temperature and vapor fields and growth or evaporation rates is explained. The nonsteady-state kinetics for changing surface conditions is treated, taking a freezing supercooled droplet as an example. It is shown that a freezing supercooled droplet generates a wave of supersaturation around it. The head of the wave moves outward to a position about one droplet diameter away from the surface, and remains there until the droplet is completely frozen. Satellite droplet formation around a freezing droplet is explained by nucleation on unactivated condensation nuclei under the influence of this supersaturation. It is suggested that the supersaturation near a droplet which freezes may activate nearby ice nuclei which would be inactive under normal environmental conditions in a cloud.

1. Introduction

The rate of growth or evaporation of water droplets is of great importance in cloud physics. These processes are customarily treated by using a quasi-steady-state (QSS) assumption to describe the vapor and temperature fields in the droplet environment, although these fields are inherently time dependent. When a droplet grows or evaporates relatively slowly by molecular diffusion of water vapor and heat, the QSS assumption is known to be quite good. However, the accuracy decreases as environmental conditions change more and more rapidly. Such rapid changes do occur in the atmosphere, although relatively infrequently, but are more frequently encountered in the laboratory. When one faces a problem involving the nonsteady-state (NSS) behavior of droplets, it is often desirable to be able to evaluate the extent of the deviation from QSS conditions.

There have been numerous attempts in the past to describe such phenomena, but due to the complexity of the subject, rigorous treatments were obtained only by making unrealistic assumptions, such as treating only the vapor diffusion field while assuming an infinite rate of heat transfer between droplets and environment. Fukuta and Walter (1970) showed that such a treatment introduces large errors in the description of droplet growth or evaporation. However, Nix and Fukuta (1973) have obtained closed analytical solutions for this problem when the form of the rates of environmental changes is prescribed. The method of solution involves a lengthy mathematical treatment, and it may be worthwhile to make the results convenient for use in cloud physics studies.

The purpose of this paper is, therefore, twofold. First, we shall briefly review the general features of the results of our recent analysis on NSS droplet kinetics in which environmental conditions change rapidly with time (we shall call this *NSS of the first kind*) and explain how to apply the results to problems in cloud physics. Second, we shall analyze another NSS problem of droplet kinetics in which the boundary conditions at the droplet surface, rather than those in the environment, change rapidly with time. We call this *NSS of the second kind*. The most interesting example is the freezing of a supercooled droplet. We shall describe the vapor and temperature fields surrounding a freezing droplet. From this analysis, we shall examine the intensity, the extent in space, the duration and the movement of the supersaturation wave created around the freezing droplet, and discuss the role played in activation of condensation and ice nuclei.

[1] Presented at the International Cloud Physics Conference, London, 21–26 August 1972.

[2] Present affiliation: Metallurgie der Kernbrennstoffe, Rhein-Westf. Technische Hochschule, Aachen, W. Germany.

2. Nonsteady-state theory of droplet growth under a rapid environmental change

When the environment of a stationary droplet changes rapidly, transient changes appear in the state of the droplet itself and in the surrounding vapor and temperature fields. The environmental field changes can be described in terms of fluxes and sources (or sinks) for the corresponding field quantities. The fields themselves, however, must satisfy the boundary conditions at the droplet surface and in the distant environment.

In our treatment (Nix and Fukuta, 1973) the vapor and temperature fields are continuous for $r_s \leqslant r < \infty$, where r is the radial coordinate and r_s the droplet radius. Thus, the boundary conditions at the droplet surface are Maxwellian (see Fukuta and Walter, 1970). At time $t=0$, the system is in equilibrium, with temperature T_0, vapor density ρ_0, and 100% relative humidity everywhere. A variety of modes for the environmental change is possible; in order to solve the problem, we must prescribe the way in which the environment changes. We assume that the environmental conditions change exponentially with time, *viz.*

$$M = W_\rho \exp(-\kappa_\rho t), \tag{1a}$$

$$E = W_T \exp(-\kappa_T t), \tag{1b}$$

where M and E are source functions for mass and heat, W_ρ and W_T the maximum rates of change for the respective sources, and κ_ρ and κ_T the respective time constants. An exponentially varying environmental change is applicable to many situations in the laboratory and in nature.

We assume that in a small temperature range about T_0, the water vapor density ρ_s at the droplet surface varies linearly with the surface temperature T_s:

$$\rho_s = \rho_0[1+n(T_s-T_0)] \tag{2}$$

at the droplet surface; and the latent heat released by the condensing vapor is assumed equal to that carried away by conduction to the environment:

$$LD(\partial\rho/\partial r)_{r=r_s} = -K(\partial T/\partial r)_{r=r_s}, \tag{3}$$

where L is the latent heat of condensation, D the coefficient of diffusion of water vapor in air, and K the thermal conductivity of air.

Thus, the equations of heat conduction and diffusion for this problem, in spherical coordinates, are

$$\frac{\partial}{\partial t} r\rho(r,t) = D\frac{\partial^2}{\partial r^2} r\rho(r,t) + rM, \tag{4a}$$

$$\frac{\partial}{\partial t} rT(r,t) = a\frac{\partial^2}{\partial r^2} rT(r,t) + r\left(\frac{E}{c\rho_g}\right), \tag{4b}$$

where c and ρ_g are the specific heat and density of air, respectively, and $a=K/(c\rho_g)$ is the thermal diffusivity of air. The Laplace integral transformation was used to solve (4a, b) subject to (1a, b), (2) and (3). The solutions obtained are as follows:

$$\rho(r,t) = \rho_0 + \frac{W_\rho}{\kappa}(1-e^{-v^2}) - C_\rho\left(\frac{r_s}{r}\right)\varphi(x_\rho,y), \tag{5a}$$

$$T(r,t) = T_0 + \frac{W_T}{\kappa c\rho_g}(1-e^{-v^2}) + C_T\left(\frac{r_s}{r}\right)\varphi(x_T,y), \tag{5b}$$

where

$$\left.\begin{aligned} \varphi(x,y) &= \operatorname{erfc}x - e^{-x^2}\operatorname{Re}[\exp(x+iy)^2 \operatorname{erfc}(x+iy)] \\ C_\rho &= \left(1+\frac{LD\rho_0 n}{K}\right)^{-1}\left(\frac{W_\rho}{\kappa} - \frac{\rho_0 n W_T}{c\rho_g \kappa}\right) \\ C_T &= \left(\frac{K}{LD}+\rho_0 n\right)^{-1}\left(\frac{W_\rho}{\kappa} - \frac{\rho_0 n W_T}{c\rho_g \kappa}\right) \end{aligned}\right\},$$

and $x_\rho = \frac{1}{2}(r-r_s)(Dt)^{-\frac{1}{2}}$, $x_T = \frac{1}{2}(r-r_s)(at)^{-\frac{1}{2}}$ and $y=(\kappa t)^{\frac{1}{2}}$. We have set $\kappa_\rho = \kappa_T = \kappa$. From (2) we see that $\rho_0 n$ is the slope of the Clausius-Clapeyron equation, $d\rho_s/dT_s$, at temperatures near T_0.

When the Maxwellian QSS treatment is applied to droplet growth under changing environmental conditions, the temperature and vapor density fields are also given by (5a, b), but with the function φ set equal to unity. Thus, the NSS effects on vapor and temperature fields are contained in φ. Fig. 1 shows the dependency of φ on the dimensionless variables x and y. It is apparent from the figure that NSS effects become important when x is large and y is small. Using this plot of $\varphi(x,y)$, one can quantitatively estimate the errors in the vapor and temperature fields arising from the QSS treatment.

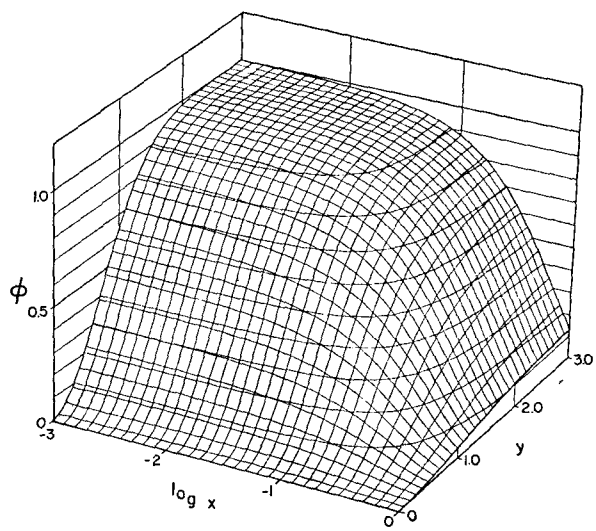

FIG. 1. φ function plotted against $\log_{10} x$ and y.

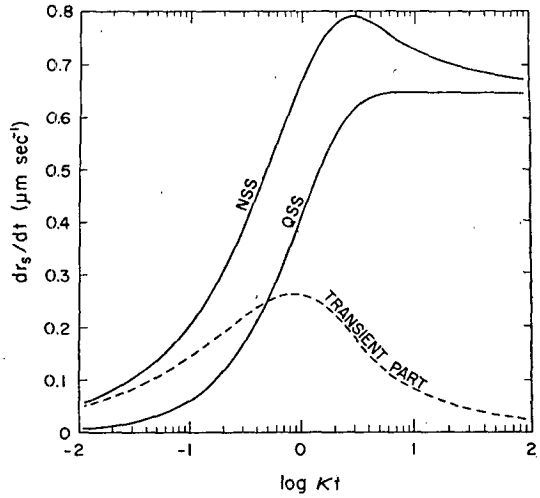

FIG. 2. Radial growth rates of a droplet 100 μm in radius during the cooling from 15 to 0C under $\kappa=1000$ sec^{-1}.

The mass growth rate of a droplet, which is often the main interest in cloud physics, was obtained as

$$\frac{dm}{dt}=4\pi r_s DC_\rho\left\{[1-\exp(-y^2)]+2r_s\left(\frac{\kappa}{D\pi}\right)^{\frac{1}{2}}\exp(-y^2)\int_0^y\exp(u^2)du\right\}. \quad (6)$$

Fig. 2 shows an example of radial growth rates estimated from (6). The broken line shows the transient effect due to the last term. One of the main results of our treatment is that simulation of a rapid NSS growth by applying the QSS theory in a stepwise manner, which many workers employed in the past, results in the QSS line in the figure, clearly revealing a serious error expressed by the transient part. Fig. 3 shows the relative mass growth rate deviation between the NSS and QSS with respect to the nondimensional time κt, with κ as the parameter.

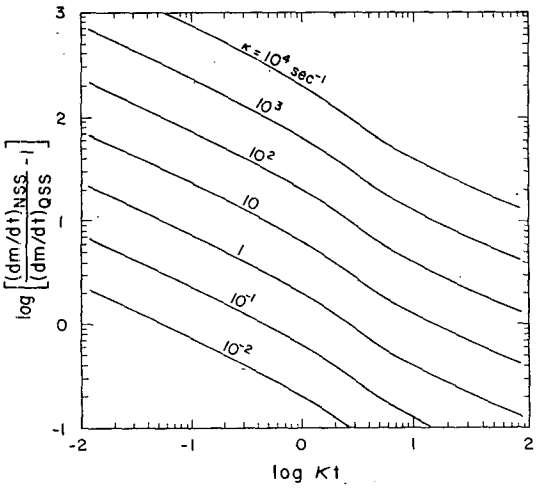

FIG. 3. Error in dm/dt vs κt with κ as the parameter.

3. Supersaturation around a freezing supercooled droplet

Freezing of a supercooled droplet presents an interesting problem in cloud microphysics. First, it is an example of the NSS kinetics of the second kind. Second, the process generates a supersaturation wave which spreads into and profoundly affects the surrounding environment.

While investigating the freezing behavior of a supercooled drop experimentally, Dye and Hobbs (1968) observed that a cloud of small droplets appeared in the vicinity of the freezing drop. They adopted a simple theoretical model to this phenomenon, explained formation of regions of high supersaturation with respect to water which should be produced within a distance a few radii from the center of the freezing drop, and concluded that the cloud of small droplets formed by condensation in the region of high supersaturation. Cheng (1970) also reported satellite droplet formation around a freezing supercooled drop, but he assumed the satellite droplets were ejected from the freezing drop. The suggested mechanism was criticized by Hobbs (1971) and shown experimentally by Rosinski *et al.* (1972) to be not possible.

In this section, we shall develop the NSS kinetics of a droplet of the second kind and quantitatively show how the supersaturation wave is generated, moves, and contributes to the activation of cloud condensation nuclei surrounding the freezing droplet. This supersaturation wave is also important for activation of ice nuclei in the environment of a freezing droplet.

a. Physical concept

The mathematical treatment is based on the following physical model. At first we consider this model in a heuristic way.

Let us assume a stationary supercooled water droplet with a radius r_s in an environment saturated with respect to water. The vapor density and temperature are T_∞ and ρ_∞, respectively, all over the space including the droplet, and the saturation ratio of the vapor is unity with respect to water, for $t<0$. At $t=0$ the droplet starts freezing and releasing the latent heat

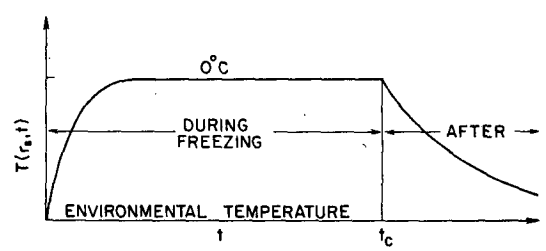

FIG. 4. Thermal behavior of a freezing droplet.

of fusion. This heat will warm up the droplet from T_∞ to T_0 [$\approx$0C] in a relatively short time. This is shown in Fig. 4. The droplet stays considerably warmer than its environment until the latent heat is exhausted by evaporation and heat conduction. This QSS condition of the droplet lasts for some time. During this time the evaporating droplet pours additional water vapor and heat into its surroundings. The release of vapor dominates over the release of heat, so that a region of supersaturation is created. The heat production ends when the droplet is entirely frozen at time t_c. After t_c, the temperature, vapor density and supersaturation all collapse very quickly, but they will not come back to the original conditions again; the temperature of the frozen droplet remains warmer than the environment. We split this process into two parts: during freezing and after freezing.

b. During freezing

The transport processes of water vapor and heat are basically the same as those in Section 2, but without any source functions in the present case. Therefore, the differential equations are

$$\frac{\partial}{\partial t} r\rho(r,t) = D\frac{\partial^2}{\partial r^2} r\rho(r,t), \tag{7a}$$

$$\frac{\partial}{\partial t} rT(r,t) = a\frac{\partial^2}{\partial r^2} rT(r,t), \tag{7b}$$

with $0 \leqslant t \leqslant t_c$ and $r_s \leqslant r \leqslant \infty$. The initial conditions are

$$\rho(r,0) = \rho_\infty \quad \text{and} \quad T(r,0) = T_\infty. \tag{8a,b}$$

The condition at the droplet surface needs to be prescribed. For the same reason we discussed in Section 2, we introduce an exponential form for the temperature:

$$T(r_s,t) - T_\infty = (T_0 - T_\infty)(1 - e^{-\kappa t}), \tag{9}$$

with $0 \leqslant t \leqslant t_c$, which is a reasonable representation for the sharp temperature rise of the droplet at the beginning of freezing; κ in (9) is yet to be determined. If we assume that the droplet will come to $T_0 \approx$0C in the time taken for an ice dendrite to grow from one side of the droplet to the opposite side, then from the data of Pruppacher (1967), we obtain

$$\kappa = \frac{0.4(T_0 - T_\infty)}{r_s}. \tag{10}$$

Furthermore it turns out that the exact value of κ is largely unimportant because it does not affect the results much; when we changed the value in (10) by one order of magnitude smaller or larger, the maximum supersaturation changed to 14.7% and 14.9%, respectively.

For the other condition at the surface of the droplet, i.e., the saturation vapor density with respect to water, we employ a quadratic approximation

$$\rho_{\text{sat}}(T) = \rho_\infty(1 + nT + mT^2), \tag{11}$$

where constants n and m can be determined by the temperature at the surface during the change. The error of (11) over the temperature range 0 to $-$15C is less than 1%. Replacing T in (11) with $T(r_s,t) - T_\infty$ given by (9) gives the inner boundary or droplet surface condition for (7a). The outer boundary conditions are

$$\rho(\infty,t) = \rho_\infty \quad \text{and} \quad T(\infty,t) = T_\infty. \tag{12a,b}$$

The problem is now to solve (7a) and (7b) with the boundary conditions (8a, b), (9), (11) and (12a, b). The mathematical treatment of this derivation is given in Appendix A.

The expressions obtained for the vapor density and temperature fields are

$$\rho(r,t) - \rho_\infty = (T_0 - T_\infty)\frac{r_s}{r}[n + m(T_0 - T_\infty)]\varphi(x_\rho, y) + m(T_0 - T_\infty)[\varphi(x_\rho, y) - \varphi(x_\rho, \sqrt{2}y)], \tag{13a}$$

$$T(r,t) - T_\infty = (T_0 - T_\infty)\frac{r_s}{r}\varphi(x_T, y). \tag{13b}$$

Use of a further approximation with $m=0$ in (13a) yields a simpler expression. The supersaturation distribution can be obtained, using (13a), (13b) and (11), as

$$S(r,t) - 1 = \frac{\rho(r,t)}{\rho_{\text{sat}}[T(r,t)]} - 1. \tag{14}$$

c. Freezing time

By the time t_c, freezing of the droplet is completed. During the process, the latent heat of fusion must be exhausted from the frozen droplet or ice sphere by sublimation of water vapor and heat conduction from it, except for a small amount of heat stored in the ice. Therefore,

$$\tfrac{4}{3}\pi r_s^3 \rho_l L_f = \int_0^{t_c} \left\{ \tfrac{4}{3}\pi r_s^3 \rho_i c_i \frac{d}{dt} T(r_s,t) - 4\pi r_s^2 \left[K\frac{d}{dr} T(r,t) + LD\frac{d}{dr}\rho(r,t) \right]_{r=r_s} \right\} dt, \tag{15}$$

where ρ_l, L_f, ρ_i and c_i denote the liquid density, latent heat of fusion, ice density, and specific heat of ice, respectively. The time t_c may be determined from (15) by inserting (13a, b). Appendix B shows the mathematical procedure. Here, we only present a truncated but valid result to estimate t_c, i.e.,

$$\tfrac{4}{3}\pi r_s^3 \rho_l L_f = d_1 t_c^{\frac{1}{2}} + d_2 t_c + d_3 + d_4, \tag{16}$$

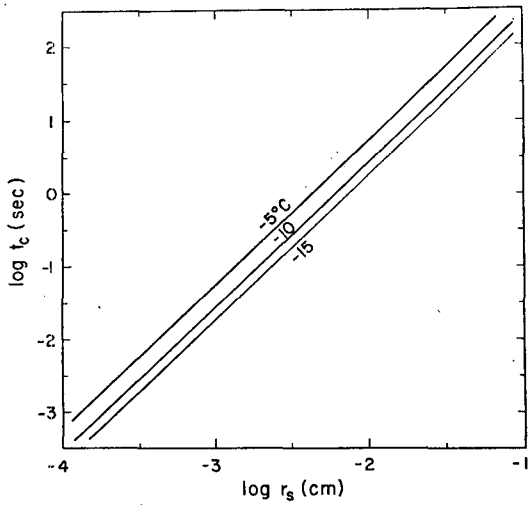

FIG. 5. Time of freezing t_c vs droplet radius r_s.

where d_1, d_2, d_3, d_4 are constants with respect to t_c which are defined in Appendix B. In Fig. 5, t_c values estimated from (16) are plotted for three different supercooling temperatures. It is apparent from the figure that $t_c \propto r_s^2$, approximately.

d. After freezing

When $0 \leqslant t \leqslant t_c$, we assume the temperature of the droplet surface to be in the form of (9). After freezing where $t_c \leqslant t < \infty$, such an assumption is no longer possible. Therefore, for the analysis after freezing, we introduce the new time variable, $t' = t - t_c$.

The differential equations for both temperature and vapor density fields are the same as (7a, b) if t is replaced by t'. The initial conditions are given by (13a, b) with $t = t_c$, or by the QSS equations, if $t_c \gg 1/\kappa$, which is always the case for $r_s > 5$ μm, *viz.*

$$\rho(r,0) = \frac{r_s}{r}(T_0 - T_\infty) + T_\infty, \tag{17a}$$

$$T(r,0) = \frac{r_s}{r}(\rho_0 - \rho_\infty) + \rho_\infty, \tag{17b}$$

where $T_0 \approx 0$C and ρ_0 is the saturation vapor density at T_0.

At the ice sphere surface, the first boundary condition one has to consider is the heat balance; the rate of heat loss inside the sphere matches the rates of heat release from the surface by conduction and vapor sublimation, or

$$\tfrac{4}{3}\pi r_s^3 \rho_i c_i \frac{d}{dt'} T(r_s,t') = 4\pi r_s^2 \left[K \frac{\partial}{\partial r} T(r,t') + L_s D \frac{\partial}{\partial r} \rho(r,t') \right]_{r=r_s}, \tag{18}$$

where L_s is the latent heat of sublimation. Although neglect of the heat capacity of the droplet was permissible in Section 2 since the stored heat was small compared with the latent heat of condensation, it is no longer permissible after freezing has ended. In this case, the heat stored in the ice sphere directly controls the process.

The second boundary condition at the ice surface is the saturation vapor density as a function of temperature. This time we take the linear relation

$$\rho(r_s,t') = \rho_0\{1 + n_i[T(r_s,t') - T_0]\}. \tag{19}$$

In addition, (12a) and (12b) are valid in the distant environment. The mathematical procedure of solving for the fields after freezing is treated in Appendix C; the solutions are

$$\rho(r,t') - \rho(r,0) = n_i \rho_0 \frac{b_4}{b_3} \frac{r_s}{r} \left\{ \operatorname{erfc} x_\rho + \frac{1}{\operatorname{Im} u} \operatorname{Im}[\bar{u} \exp \xi_\rho^2 \operatorname{erfc} \xi_\rho] \right\}, \tag{20a}$$

$$T(r,t') - T(r,0) = \frac{b_4}{b_3} \frac{r_s}{r} \left\{ \operatorname{erfc} x_T + \frac{1}{\operatorname{Im} u} \operatorname{Im}[\bar{u} \exp \xi_T^2 \operatorname{erfc} \xi_T] \right\}, \tag{20b}$$

where $\xi = x + u\sqrt{t'}$, and b_1, b_3 and u are constants defined in Appendix C. The supersaturation can be obtained from (20a) and (20b) as in (14) except with t' in place of t.

The fields of water vapor density, temperature and supersaturation are plotted in Fig. 6 with the time as a parameter, for a supercooled droplet of 50 μm radius at an initial temperature of -15C. The fields during freezing are shown on the left-hand side, and those after freezing on the right. A few interesting features may be seen in the figure. First of all, within an initial 4-msec period, the vapor density and temperature fields rapidly establish steady profiles near the surface, and thereafter the fields spread outward till the QSS profiles are achieved. The supersaturation field swells up and reaches its maximum height of about 15% with respect to water within this 4-msec period. Then the maximum in the supersaturation field moves slightly outward to a position approximately one droplet diameter away from the droplet surface and stays there. The zone in which supersaturation with respect to water exceeds 2% will expand to include a spherical volume of about 30 droplet radii or 1.5 mm. Evaluation of (13a, b) and (14) for other initial conditions shows that the values of the maximum supersaturation are almost independent of the droplet radius but are strongly affected by the supercooling temperature,

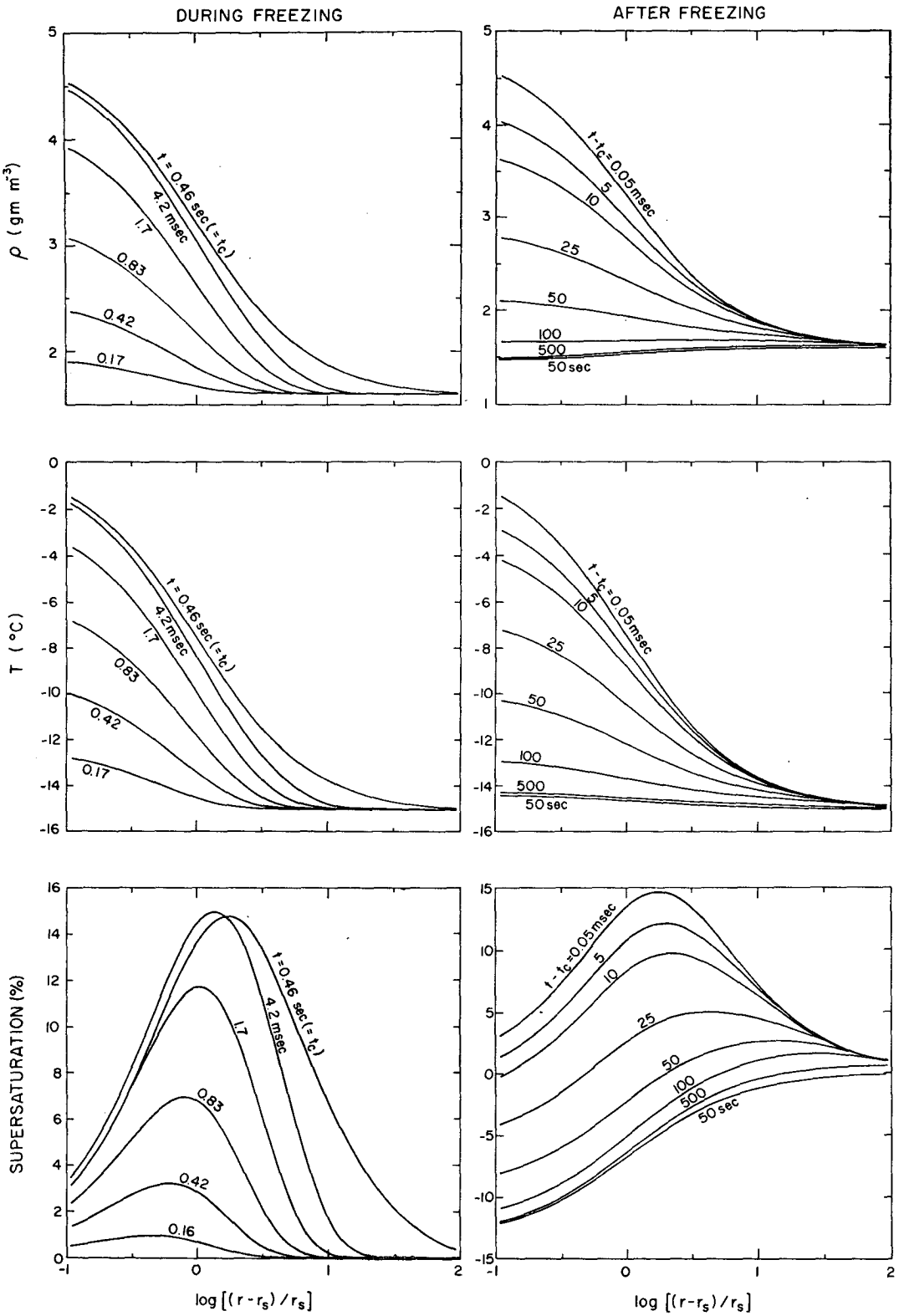

FIG. 6. Field changes for the vapor density, temperature and supersaturation during and after freezing of a supercooled droplet of 50 μm in radius placed in an environment saturated with respect to water at -15C: $\kappa = 1200$ sec^{-1}.

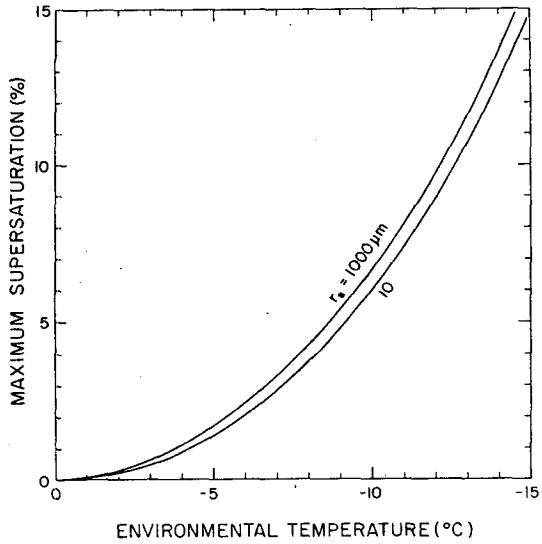

FIG. 7. Maximum supersaturation vs temperature of the environment saturated with respect to water.

$T_\infty - T_0$. This tendency may be seen in Fig. 7 for droplets of radii 10 and 1000 μm.

e. Discussion

Freezing of a supercooled cloud droplet not only gives a rare example of the NSS kinetics of a droplet of the second kind, in which the surface condition changes with respect to time, but also generates a spherical wave of supersaturation. The maximum supersaturation at the wave head readily exceeds the maximum supersaturation in the cloud, which is on the order of 1% with respect to water. The sphere of influence becomes rather large since the addition of a small amount of water vapor into the environment makes the vapor density much higher than the saturation vapor density which is relatively low in the temperature zone in question. It is obvious that the larger the droplet, the greater the volume of the sphere of influence. A freezing cloud droplet easily spreads its influence to a distance of the order of 1 mm from its surface. As the average spacing between cloud droplets in many clouds is also on the order of 1 mm, within the sphere of influence one is not likely to find any droplets which may interfere with the supersaturation field. For this reason, the computed supersaturation must be real and not nominal. Within this region, any supersaturation dependent phenomena, such as nucleation of cloud droplets and ice crystals, will be strongly affected.

The satellite droplet formation observed by Dye and Hobbs (1968) and Cheng (1970) can be explained by the effect of this supersaturation which nucleates droplets on unactivated cloud nuclei, as first suggested by Dye and Hobbs.

Another possible interesting effect is the self-induced mode of ice nucleus activation. When a plume of ice nuclei spreads in a supercooled cloud whose temperature is warm, the dominant mechanism there is contact or condensation freezing, at least at the beginning of the interaction. However, when freezing of a droplet takes place, a sphere of supersaturation developes and it is possible to activate sublimation as well as condensation-freezing nuclei, if they exist, which are unable to activate under the normal cloud supersaturation. This phenomenon deserves further experimental investigation, and may be important in cloud seeding where the number concentration of nuclei is high. It has already been shown that the supersaturation, although created by evaporative cooling of an organic drop, does activate ice nuclei (Fukuta, 1965).

It should also be pointed out that a growing hailstone exerts a similar influence of supersaturation to the cloud environment although the mechanism of heat generation and the aerodynamic condition around it are different. In this case, however, the interference from the cloud droplets is expected to be greater.

Acknowledgments. We are thankful for the partial support of the Environmental Systems and Resources Division, National Science Foundation, under Grant CA-29525, and one of us (N. N.) gratefully acknowledges the grant from Deutcher Akademischer Austausch Dienst (No. 4304027012) to perform this study. The calculations were done at the Computing Facility of the National Center for Atmospheric Research, which is sponsored by the National Science Foundation. We are also indebted to Dr. M. N. Plooster for discussion of the subjects involved.

APPENDIX A

Derivation of Field Expressions for the Vapor Density and Temperature During Freezing

Using the Laplace transformation with the notation

$$P(r,s)=\int_0^\infty \rho(r,t)e^{-st}dt$$

$$\theta(r,s)=\int_0^\infty T(r,t)e^{-st}dt, \qquad \text{(A1a, b)}$$

Eqs. (7a) and (7b) become

$$\frac{d^2}{dr^2}P(r,s)-\frac{s}{D}\left[rP(r,s)-\frac{r\rho_\infty}{s}\right]=0, \qquad \text{(A2a)}$$

$$\frac{d^2}{dr^2}\theta(r,s)-\frac{s}{a}\left[r\theta(r,s)-\frac{rT_\infty}{s}\right]=0. \qquad \text{(A2b)}$$

Solutions of (A2a) and (A2b), with the knowledge that

$P(r,s)$ and $\theta(r,s)$ are finite as $r\to\infty$, are

$$P(r,s)-\frac{\rho_\infty}{s}=\frac{A}{r}\exp\left[-\left(\frac{s}{D}\right)^{\frac{1}{2}}r\right], \tag{A3a}$$

$$\theta(r,s)-\frac{T_\infty}{s}=\frac{B}{r}\exp\left[-\left(\frac{s}{a}\right)^{\frac{1}{2}}r\right], \tag{A3b}$$

where A and B are to be determined from the boundary conditions. Therefore, we insert (9) in (11), and transform both (11) and (9), to obtain

$$P(r_s,s)-\rho_\infty=\rho_\infty(T_0-T_\infty)\left[\frac{n+m(T_0-T_\infty)}{s}-\frac{n+2m(T_0-T_\infty)}{s+\kappa}+\frac{m(T_0-T_\infty)}{s+2\kappa}\right], \tag{A4a}$$

$$\theta(r_s,s)-T_\infty=(T_0-T_\infty)\left(\frac{1}{s}-\frac{1}{s+\kappa}\right). \tag{A4b}$$

Replacing r with r_s in (A3a) and (A3b), and comparing the results with (A4a) and (A4b), gives

$$A=(T_0-T_\infty)\rho_\infty\left[\frac{n+m(T_0-T_\infty)}{s}-\frac{n+2m(T_0-T_\infty)}{s+\kappa}+\frac{m(T_0-T_\infty)}{s+2\kappa}\right]r_s\exp\left[\left(\frac{s}{D}\right)^{\frac{1}{2}}r_s\right], \tag{A5a}$$

$$B=(T_0-T_\infty)\left(\frac{1}{s}-\frac{1}{s+\kappa}\right)r_s\exp\left[\left(\frac{s}{a}\right)^{\frac{1}{2}}r_s\right]. \tag{A5b}$$

Substituting (A5a) in (A3a) and (A5b) in (A3b), we obtain the solution of (A2a) and (A2b), i.e.,

$$P(r,s)-\frac{\rho_\infty}{s}=(T_0-T_\infty)\rho_\infty\frac{r_s}{r}\left[\frac{n+m(T_0-T_\infty)}{s}-\frac{n+2m(T_0-T_\infty)}{s+\kappa}+\frac{m(T_0-T_\infty)}{s+2\kappa}\right]\times\exp\left[-\left(\frac{s}{D}\right)^{\frac{1}{2}}(r-r_s)\right], \tag{A6a}$$

$$\theta(r,s)-\frac{T_\infty}{s}=(T_0-T_\infty)\frac{r_s}{r}\left(\frac{1}{s}-\frac{1}{s+\kappa}\right)\times\exp\left[-\left(\frac{s}{a}\right)^{\frac{1}{2}}(r-r_s)\right]. \tag{A6b}$$

The inversion of (A6a) and (A6b) is performed in the normal way to give

$$\rho(r,t)-\rho_\infty=(T_0-T_\infty)\rho_\infty\frac{r_s}{r}\left\{[n+m(T_0-T_\infty)]\operatorname{erfc}\frac{r-r_s}{2\sqrt{Dt}}-\tfrac{1}{2}[n+2m(T_0-T_\infty)]e^{-\kappa t}\left[\exp\left[-i(r-r_s)\left(\frac{\kappa}{D}\right)^{\frac{1}{2}}\right]\times\operatorname{erfc}\left(\frac{r-r_s}{2\sqrt{Dt}}-i\sqrt{\kappa t}\right)+\exp\left[i(r-r_s)\left(\frac{\kappa}{D}\right)^{\frac{1}{2}}\right]\times\operatorname{erfc}\left(\frac{r-r_s}{2\sqrt{Dt}}+i\sqrt{\kappa t}\right)\right]+\tfrac{1}{2}m(T_0-T_\infty)e^{-2\kappa t}\times\left[\exp\left[-i(r-r_s)\left(\frac{2\kappa}{D}\right)^{\frac{1}{2}}\right]\operatorname{erfc}\left(\frac{r-r_s}{2\sqrt{Dt}}-i\sqrt{2\kappa t}\right)+\exp\left[i(r-r_s)\left(\frac{2\kappa}{D}\right)^{\frac{1}{2}}\right]\operatorname{erfc}\left(\frac{r-r_s}{2\sqrt{Dt}}+i\sqrt{2\kappa t}\right)\right]\right\}, \tag{A7a}$$

$$T(r,t)-T_\infty=(T_0-T_\infty)\frac{r_s}{r}\left\{\operatorname{erfc}\frac{r-r_s}{2\sqrt{at}}-\tfrac{1}{2}e^{-\kappa t}\times\left[\exp\left[-i(r-r_s)\left(\frac{\kappa}{a}\right)^{\frac{1}{2}}\right]\operatorname{erfc}\left(\frac{r-r_s}{2\sqrt{at}}-i\sqrt{\kappa t}\right)+\exp\left[i(r-r_s)\left(\frac{\kappa}{a}\right)^{\frac{1}{2}}\right]\operatorname{erfc}\left(\frac{r-r_s}{2\sqrt{at}}+i\sqrt{\kappa t}\right)\right]\right\}. \tag{A7b}$$

After introducing the dimensionless parameters x_ρ, x_T and y and rearranging, it can be shown that the imaginary parts of the total expression in (A7a) and (A7b) are identically zero and the results can be written in the form of (13a) and (13b).

APPENDIX B

Estimation of Freezing Time

To evaluate (15), we first have to determine the three derivatives

$$\frac{d}{dt}T(r_s,t),\quad\left[\frac{d}{dr}T(r,t)\right]_{r=r_s}\quad\text{and}\quad\left[\frac{d}{dr}\rho(r,t)\right]_{r=r_s}.$$

Using (A6a) and (A6b) and setting $r=r_s$, we obtain the transformed expressions for these three derivatives:

$$(T_0-T_\infty)s\left(\frac{\kappa}{s(s+\kappa)}\right),$$

$$-(T_0-T_\infty)\left(\frac{1}{s}-\frac{1}{s+\kappa}\right)\left[\frac{1}{r_s}+\left(\frac{s}{a}\right)^{\frac{1}{2}}\right],$$

$$-(T_0-T_\infty)\rho_\infty\left[\frac{n+m(T_0-T_\infty)}{s}-\frac{n+2m(T_0-T_\infty)}{s+\kappa}+\frac{m(T_0-T_\infty)}{s+2\kappa}\right]\left[\frac{1}{r_s}+\left(\frac{s}{D}\right)^{\frac{1}{2}}\right],$$

respectively. Inserting these terms into the integrand of (15) and dividing by s, we get the transformed expression of the integral:

$$\tfrac{4}{3}\pi r_s^3\rho_i c_i(T_0-T_\infty)\left[\frac{\kappa}{s(s+\kappa)}\right]+4\pi r_s^2(T_0-T_\infty)\times\left\{K\left[\frac{1}{s^2}-\frac{1}{s(s+\kappa)}\right]\left[\frac{1}{r_s}+\left(\frac{s}{a}\right)^{\frac{1}{2}}\right]+LD\rho_\infty\times\left[\frac{n+m(T_0-T_\infty)}{s^2}-\frac{n+2m(T_0-T_\infty)}{s(s+\kappa)}+\frac{m(T_0-T_\infty)}{s(s+2\kappa)}\right]\left[\frac{1}{r_s}+\left(\frac{s}{D}\right)^{\frac{1}{2}}\right]\right\}.$$

The inversion of this expression is

$$F(t)=d_1\sqrt{t}+d_2t+d_3(1-e^{-\kappa t})+d_4(1-e^{-2\kappa t})+id_5e^{-\kappa t}\operatorname{erf}(i\sqrt{\kappa t})-id_6e^{-2\kappa t}\operatorname{erf}(i\sqrt{2\kappa t}), \quad \text{(B1)}$$

with

$$\left.\begin{aligned}
d_1&=8\sqrt{\pi}r_s^2(T_0-T_\infty)\left\{\frac{K}{\sqrt{a}}+\frac{LD\rho_\infty[n+m(T_0-T_\infty)]}{\sqrt{D}}\right\}\\
d_2&=4\pi r_s(T_0-T_\infty)\{K+LD\rho_\infty[n+m(T_0-T_\infty)]\}\\
d_3&=\frac{4\pi r_s}{\kappa}(T_0-T_\infty)\{\tfrac{1}{3}r_s^2\rho_i c_i\kappa-K-LD\rho_\infty[n+m(T_0-T_\infty)]\}\\
d_4&=\frac{2\pi r_s}{\kappa}(T_0-T_\infty)^2LD\rho_\infty m\\
d_5&=4\pi r_s^2\frac{1}{\sqrt{\kappa}}(T_0-T_\infty)\left\{\frac{K}{\sqrt{a}}+\frac{LD\rho_\infty[n+2m(T_0-T_\infty)]}{\sqrt{D}}\right\}\\
d_6&=\frac{4\pi r_s^2LD\rho_\infty(T_0-T_\infty)^2m}{2\sqrt{\kappa D}}
\end{aligned}\right\}.$$

We look for the time t_c when

$$F(t_c)=\tfrac{4}{3}\pi r_s^3\rho_iL_f. \quad \text{(B2)}$$

Since $\kappa t_c\gg 1$ for not too small droplets, the terms in (B1) become

$$e^{-\kappa t_c}\approx e^{-2\kappa t_c}\approx e^{-\kappa t_c}\operatorname{erf}(i\sqrt{\kappa t_c})\approx e^{-2\kappa t_c}\operatorname{erf}(i\sqrt{2\kappa t_c})\approx 0,$$

so that (B1) can be replaced by the right-hand side of (16).

APPENDIX C

Derivation of Temperature and Vapor Density Fields after Freezing

Since the differential equations are the same as in Appendix A, the procedure of derivation is identical. We write (A3a) and (A3b) for the special initial condition given in Eqs. (17a) and (17b) as

$$P(r,s)-\frac{1}{s}\rho(r,0)=\frac{A'}{r}\exp\left[-\left(\frac{s}{D}\right)^{\frac{1}{2}}r\right], \quad \text{(C1a)}$$

$$\theta(r,s)-\frac{1}{s}T(r,0)=\frac{B'}{r}\exp\left[-\left(\frac{s}{a}\right)^{\frac{1}{2}}r\right], \quad \text{(C1b)}$$

where A' and B' are different from A and B in Appendix A because the boundary conditions given by (18) and (19) have changed. The derivatives of (C1a) and (C1b) are

$$\frac{d}{dr}P(r,s)-\frac{1}{s}\frac{d}{dr}\rho(r,0)=\frac{A'}{r}\left[\frac{1}{r}+\left(\frac{s}{D}\right)^{\frac{1}{2}}\right]\exp\left[-\left(\frac{s}{D}\right)^{\frac{1}{2}}r\right], \quad \text{(C2a)}$$

$$\frac{d}{dr}\theta(r,s)-\frac{1}{s}\frac{d}{dr}T(r,0)=\frac{B'}{r}\left[\frac{1}{r}+\left(\frac{s}{a}\right)^{\frac{1}{2}}\right]\exp\left[-\left(\frac{s}{a}\right)^{\frac{1}{2}}r\right]. \quad \text{(C2b)}$$

The transformations of (19) and (18) are

$$P(r_s,s)-\frac{1}{s}\rho_0=\rho_0n_i\left[\theta(r_s,s)-\frac{1}{s}T_0\right], \quad \text{(C3a)}$$

$$\tfrac{1}{3}\rho_ic_i[sr_s\theta(r_s,s)-r_sT_0]=\left[K\frac{d}{dr}\theta(r,s)+L_sD\frac{d}{dr}P(r,s)\right]_{r=r_s}. \quad \text{(C3b)}$$

Inserting (C1a) and (C1b) in (C3a), we obtain

$$A'\exp(-s^{\frac{1}{2}}D^{-\frac{1}{2}}r_s)=\rho_0n_iB'\exp(-s^{\frac{1}{2}}a^{-\frac{1}{2}}r_s), \quad \text{(C4)}$$

and substitution of (C1b), (C2a) and (C2b) into (C3b) and rearranging yields

$$\frac{B'}{r_s}\exp(-s^{\frac{1}{2}}a^{-\frac{1}{2}}r_s)\left[\frac{1}{3}\rho_ic_ir_ss+(Ka^{-\frac{1}{2}}+\rho_0n_iL_sD^{\frac{1}{2}})s^{\frac{1}{2}}+\frac{K+\rho_0n_iL_sD}{r_s}\right]=\frac{1}{s}\left[K\frac{d}{dr}T(r,0)+L_sD\frac{d}{dr}\rho(r,0)\right]_{r=r_s}. \quad \text{(C5)}$$

Eqs. (C4) and (C5) determine A' and B'. In (C5) we denote the constants as

$$\left.\begin{aligned} b_1&=\tfrac{1}{3}\rho_i c_i r_s \\ b_2&=Ka^{-\frac{1}{2}}+\rho_0 n_i L_s D^{\frac{1}{2}} \\ b_3&=\frac{1}{r_s}(K+\rho_0 n_i L_s D) \\ b_4&=\left[K\frac{d}{dr}T(r,0)+L_s D\frac{d}{dr}\rho(r,0)\right]_{r=r_s} \end{aligned}\right\}. \quad \text{(C6)}$$

Solving (C4) and (C5), A' and B' are

$$A'=\frac{\rho_0 n_i b_4 r_s}{s(b_1 s+b_2 s^{\frac{1}{2}}+b_3)}\exp(s^{\frac{1}{2}}D^{-\frac{1}{2}}r_s), \quad \text{(C7a)}$$

$$B'=\frac{b_4 r_s}{s(b_1 s+b_2 s^{\frac{1}{2}}+b_3)}\exp(s^{\frac{1}{2}}a^{-\frac{1}{2}}r_s). \quad \text{(C7b)}$$

Substituting (C7a) in (C1a) and (C7b) in (C1b) we can obtain the transformed solutions. When $b_1\neq 0$ and $b_2^2\neq 4b_1b_3$, (C7b) can be written as

$$B=\frac{b_4 r_s}{b_1(u-\bar{u})s}\left(\frac{1}{s^{\frac{1}{2}}+\bar{u}}-\frac{1}{s^{\frac{1}{2}}+u}\right)\exp(s^{\frac{1}{2}}a^{-\frac{1}{2}}r_s), \quad \text{(C8)}$$

where

$$u=\frac{1}{2b_1}[b_2+i(4b_1b_3-b_2^2)^{\frac{1}{2}}], \quad \text{(C9)}$$

and $\bar{u}$ is the complex conjugate of u.

The inversion of (C1b) is then

$$\begin{aligned} T(r,t)-T(r,0)=\frac{r_s}{r}\frac{b_4}{b_1(u-\bar{u})}\Bigg[&\frac{1}{\bar{u}}\{\operatorname{erfc}x_T \\ &-\exp[\bar{u}(r-r_s)a^{-\frac{1}{2}}+u^{-2}t]\operatorname{erfc}(x_T+ut^{\frac{1}{2}})\} \\ &-\frac{1}{u}\{\operatorname{erfc}x_T-\exp[u(r-r_s)a^{-\frac{1}{2}}+u^2t] \\ &\times\operatorname{erfc}(x_T+ut^{\frac{1}{2}})\}\Bigg]. \end{aligned} \quad \text{(C10)}$$

With $e^{\bar{z}^2}=\overline{e^{z^2}}$ and $\operatorname{erfc}\bar{z}=1-\operatorname{erf}\bar{z}=1-\overline{\operatorname{erf}z}$, it can be shown that (C10) is identical with (20b). A similar treatment leads to (20a).

REFERENCES

Cheng, R. J., 1970: Water drop freezing: Ejection of microdroplets. *Science*, **170**, 1395–1396.

Dye, J. E., and P. V. Hobbs, 1968: The influence of environmental parameters on the freezing and fragmentation of suspended water drops. *J. Atmos. Sci.*, **25**, 82–96.

Fukuta, N., 1965: Activated ice nucleation by sprayed organic solutions. *J. Atmos. Sci.*, **22**, 207–211.

——, and L. A. Walter, 1970: Kinetics of hydrometeor growth from a vapor spherical model. *J. Atmos. Sci.*, **27**, 1160–1172.

Hobbs, P. V., 1971: Microdroplets and water freezing. *Science*, **173**, 849–850.

Nix, N., and N. Fukuta, 1973: Nonsteady-state theory of droplet growth. *J. Chem. Phys.*, **58**, 1735–1740.

Pruppacher, H. R., 1967: Interpretation of experimentally determined growth rates of ice crystals in supercooled water. *J. Chem. Phys.*, **47**, 1807–1813.

Rosinski, J., G. Langer and C. T. Nagamoto, 1972: On the ejection of microdroplets from the surface of a freezing water drop. *J. Appl. Meteor.*, **11**, 405–406.